

Joe Grames
March 10, 2016

Introduction

Measurements

72. 76. 80. 86. 89. 90. 93. 99. STA 108

R028

UNDEFLECTED

MHE0L01V
VBV0L01B
(ILM0L01B)
MQS0L01A
MHB0L01AH

MQJ0L02
IPM0L02
MHB0L02
MDL0L02
MHB0L02A
MHB0L02B
MBH0L03
MQJ0L03
IPM0L03

MHE0L02H

MOD5D00
IPM5D00
MOD5D01
IPM5D01

DEFLECTED

02B
02BH
0L02BV

○ BPM's
✕ STEERING COILS
⚡ SRF CAVITY
◇ QUAD
■ DIPOLE

Fig. 1. Picture shows the layout and names of the relevant beam line elements.

Additional horizontal steering coils were needed to address systematic effects. First, three steering coils (MHB0L02A, MHB0L02B, MBH0L03) were required to compensate the ~ 0.5 G vertically downward component of stray magnetic field spanning the injector area; these steering coils remained constant throughout all 5 measurements. Without the steering coils the beam would progressively deflect until reaching the beam pipe. Second, two steering coils (MBH0L01, MHB0L02) *upstream* of the spectrometer were used to correct for both the RF cavity dipole mode and stray field *between* the cryo-unit and spectrometer region. These two steering coils took on modestly different values for the five gradient settings because the size of the strength of the cavity dipole field and the beam momentum changed for each energy setting. These steering coils were set to null the horizontal beam position at the un-deflected monitors (IPM0L02, IPM0L03). The steering coils (MBH5D00H, MBH5D00AH) in the deflected beam line remained 0.0 G-cm for all measurements because this beam line is better shield from stray magnetic field and is shorter. It is worthwhile to mention that only the spectrometer dipole magnet changed value between each un-deflected and deflected measurement.

Recorded values of the cavity gradient, steering coils, spectrometer dipole, and beam position monitors for all 5 energies studied are summarized in Table 1.

Table 1. The cavity gradient (MV/m), steering coil currents (mA), spectrometer dipole field integral (G-cm) and beam position monitor readings (mm) for the experiment are listed. Beam positions are reported in a left-handed system (x =right, y =up, z =forward).

Conditions for individual measurements						Undeflected			Deflected		
R028	MBH0L01	MHB0L02	MHB0L02A	MHB0L02B	MBH0L03	MDL0L02	IPM0L02.XPOS	IPM0L03.XPOS	MDL0L02	IPM5D00.XPOS	IPM5D01.XPOS
MV/m	mA	mA	mA	mA	mA	G-cm	mm	mm	G-cm	mm	mm
3.35	-325.00	-292.00	-214.54	-0.03	-342.83	0.00	0.03	0.22	7109.57	0.00	3.50
3.74	-327.00	-293.00	-214.54	-0.03	-342.83	0.00	0.08	0.17	7384.34	0.01	3.67
4.12	-329.00	-292.00	-214.54	-0.03	-342.83	0.00	0.06	0.15	7646.01	0.00	4.06
4.50	-332.00	-286.00	-214.54	-0.03	-342.83	0.00	-0.02	0.00	7927.59	0.00	3.89
4.89	-333.00	-287.00	-214.54	-0.03	-342.83	0.00	0.05	0.21	8185.00	0.03	3.85

Uncorrected Electron Momenta : ideal orbit and TOSCA model

The MDL0L02 spectrometer dipole magnetic field measurements and corresponding TOSCA model is described in [4]. The model with default BH curve agrees with the straight-line on-axis magnetic field measurement within 0.1% [4] level. The model was used to generate the straight-line magnetic field integral corresponding to a deflecting an electron beam of momentum P (MeV/c) by $+25.0^\circ$ into the ideal diagnostic beam line. A 5th order polynomial applied to the model with corresponding coefficients shown below is plotted over the region of interest for the experiment in Fig. 2,

$$BL = M_0 + M_1 P + M_2 P^2 + M_3 P^3 + M_4 P^4 + M_5 P^5$$

$$\begin{aligned} M_0 &= +4.811 \\ M_1 &= -1416.2 \\ M_2 &= +1.2399 \\ M_3 &= -0.1646 \\ M_4 &= +0.009795 \\ M_5 &= -0.00021257 \end{aligned}$$

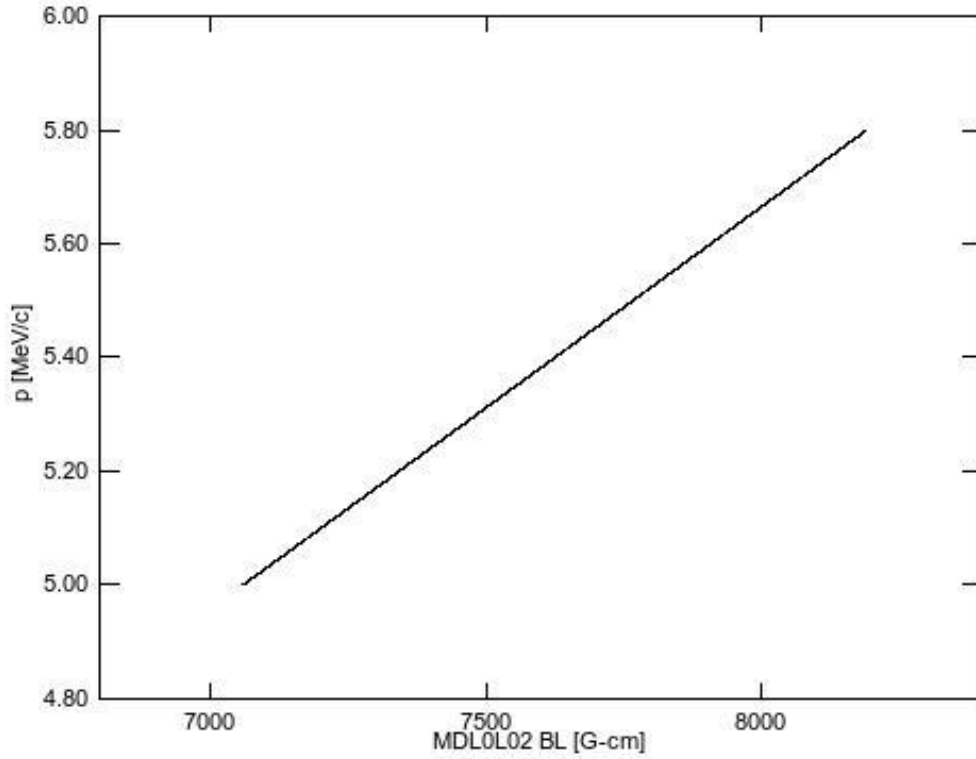


Fig. 2. Plot of momenta vs. straight-line field integral determined by TOSCA model of dipole MDL0L02 to deflect an electron beam by +25.0°.

A solution of this polynomial for the corresponding energies is given in Table 2.

Table 2. Table of momenta for 5 energies studied according to model of MDL0L02. The uncertainty of 0.1% is given by [4] as the relative agreement between model and measurement.

R028	MDL0L02	P	dP
MV/m	G-cm	MeV/c	MeV/c
3.35	7109.57	5.035	0.005
3.74	7384.34	5.229	0.005
4.12	7646.01	5.415	0.005
4.50	7927.59	5.614	0.006
4.89	8185.00	5.797	0.006

Corrected Beam Momenta: model orbit with stray field and steering coils

The beam momentum is determined by modeling the effect of the stray magnetic field and steering coils to correct the total deflection angle. The stray magnetic field and steering coils is recursively integrated for particle tracking,

```
kick=asin(2.9980E-4*b1[k]/(p))
xp[k]=xp[k-1]+kick
x[k]=x[k-1]+xp[k]*1
```

Step 1: Model of Stray Field and Steering Coils

A survey of vertical component of the stray magnetic field was made in December 2015 (see Appendix A) and is plotted in Fig. 3 over the span IPM0L02 to IPM0L03. To demonstrate the significance of the stray field trajectories of beam momenta ranging from 4.5-6.5 MeV/c are overlaid on Fig. 3; the point is that a beam centered at IPM0L02 will exit the beam pipe ($x=1.75\text{cm}$) before reaching IPM0L03.

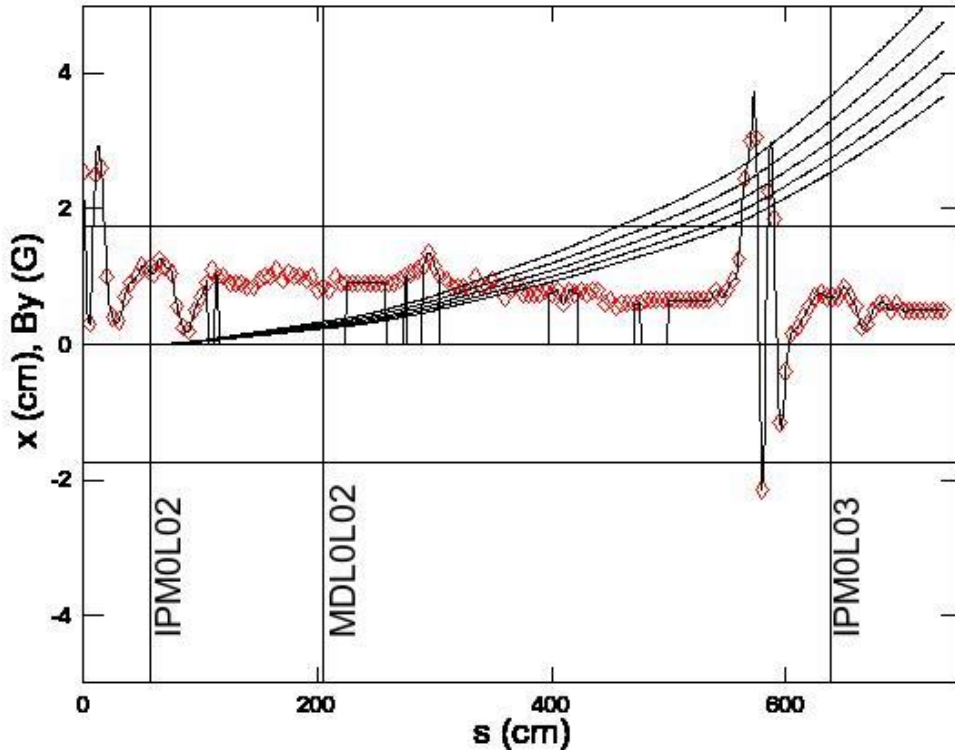


Fig. 3. Stray magnetic field measurements (red diamonds) and spline fit are used to generate $B_y(s)$ spanning IPM0L02 to IPM0L03. The field is forced to zero for regions where mu-metal shielding is added to the beam pipe. The horizontal trajectory is plotted vs. beam position over this length for momenta (4.5, 5.0, 5.5, 6.0, 6.5 MeV/c) with initial conditions IPM0L02 ($x=0\text{ cm}$, $x'=0\text{ mrad}$).

By including the steering coils used in the experiment (see Table 1), and after converting to magnetic field integral (see Appendix B), a model of the beam trajectories for the same range in momenta is more realistic (see Fig. 4); the beam is transported from IPM0L02 to IPM0L03 because the point-wise steering corrections compensate for the distributed stray field. Because deflection by both the steering coils and stray magnetic field scale linearly with beam momentum the sensitivity to be orbit is greatly minimized.

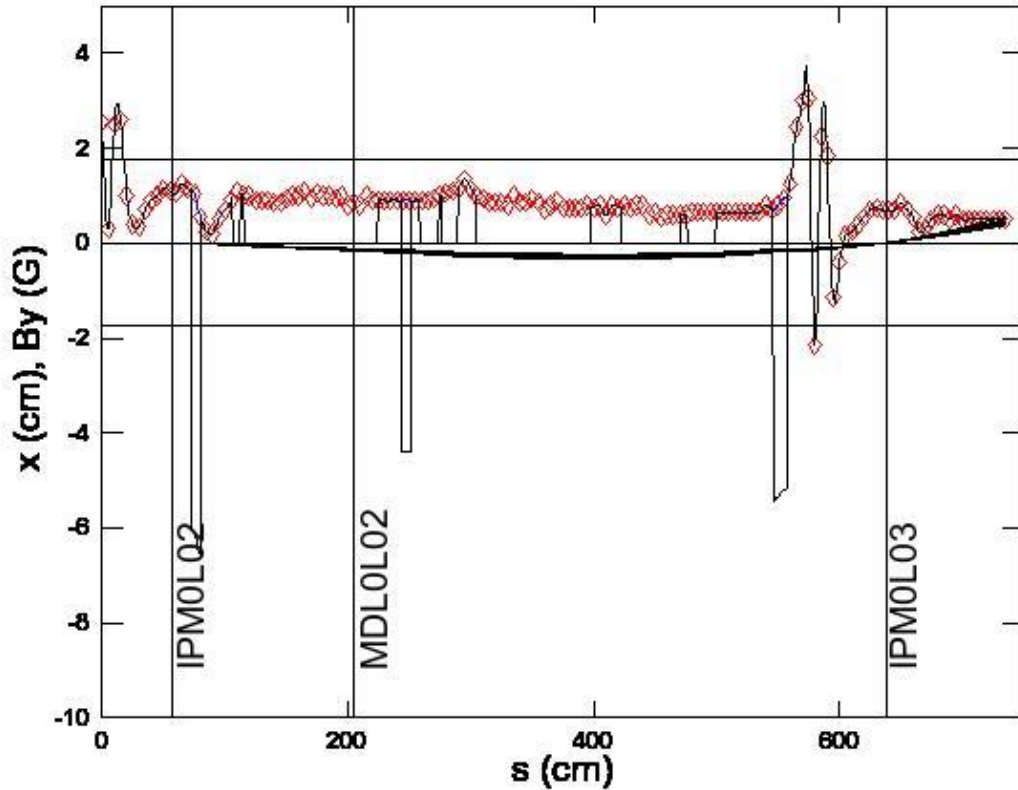


Fig. 4. Four fixed steering coils (MBH0L02, MHB0L02A, MHB0L02B, MBH0L03) are added to the model. The horizontal trajectories plotted vs. beam position over a range of momenta (4.5, 5.0, 5.5, 6.0, 6.5 MeV/c) with initial conditions IPM0L02($x=0$ cm, $x'=0$ mrad) is shown.

Step 2: BPM Analysis

Prior to the experiment each beam position monitor center was calibrated (see Appendix A) to the magnetic center of the nearest upstream quadrupole magnet. Beam monitor positions (*IPM.XPOS*) recorded during the energy measurements and reported in Table 1 are therefore relative to the quadrupoles. Corrected absolute beam positions (*IPM.XCOR*) are determined by first accounting for surveyed quadrupole positions (*QUAD.XOFF*) according to the relationship,

$$IPM.XCOR = IPM.XPOS - QUAD.XOFF.$$

Table 3. Note that the quadrupole offsets reported in [1,2] are converted from their right-handed system to the left-handed beam position monitor system.

Constant	Undelected						Deflected					
R028	IPM0L02.XPOS	MQJ0L02.XOFF	IPM0L02.XCOR	IPM0L03.XPOS	MQJ0L03A.XOFF	IPM0L03.XCOR	IPM5D00.XPOS	MQD5D00.XOFF	IPM5D00.XCOR	IPM5D01.XPOS	MQD5D01.XOFF	IPM5D01.XCOR
MV/m	mm	mm	mm	mm	mm	mm	mm	mm	mm	mm	mm	mm
3.35	0.03	-0.01	0.04	0.22	-0.24	0.46	0.00	-0.27	0.27	3.50	-0.22	3.72
3.74	0.08	-0.01	0.09	0.17	-0.24	0.41	0.01	-0.27	0.28	3.67	-0.22	3.89
4.12	0.06	-0.01	0.07	0.15	-0.24	0.39	0.00	-0.27	0.27	4.06	-0.22	4.28
4.50	-0.02	-0.01	-0.01	0.00	-0.24	0.24	0.00	-0.27	0.27	3.89	-0.22	4.11
4.89	0.05	-0.01	0.06	0.21	-0.24	0.45	0.03	-0.27	0.30	3.85	-0.22	4.07

Step 3: Application of model to determine size of correction

The orbit for each of the 5 cases may be studied separately, giving each measurement more careful inspection; however, for Mott Run II the systematically similar conditions allow for averaging the 5 measurements to compute a global average correction to the bend angle. Using Table 3 and adding uncertainties for the quadrupole survey (0.25 mm) and quad centering (0.50 mm) find,

$$\begin{aligned} \langle OL02_COR \rangle_{meas} &= 0.07 \pm 0.02 \pm 0.25 \pm 0.50 \text{ mm} = 0.07 \pm 0.56 \text{ mm} \\ \langle OL03_COR \rangle_{meas} &= 0.42 \pm 0.04 \pm 0.25 \pm 0.50 \text{ mm} = 0.42 \pm 0.56 \text{ mm} \end{aligned}$$

Using the tracking model, beam positions with total uncertainties and range of momenta 4.5-6.7 MeV/c the beam position $\langle OL03_COR \rangle_{meas}$ is satisfied within total uncertainty when conditions at IPM0L02 satisfy,

$$\begin{aligned} X &= +0.07 \pm 0.56 \text{ mm (from measurement)} \\ X' &= +0.04 \pm 0.16 \text{ mrad (from model)} \end{aligned}$$

A plot of the trajectories over range of momenta 4.5-6.7 MeV/c for these initial conditions is shown in Fig. 5. Including the uncertainty of the beam position and angle at IPM0L02 the distribution of position and angle at MDL0L02 is calculated using the model (where first uncertainty derives from conditions at IPM0L02 and IPM0L03, and second uncertainty derives from using range of momenta),

$$\begin{aligned} X &= -1.20 \pm 0.51 \pm 0.19 \text{ mm} = -1.20 \pm 0.54 \text{ mm} \\ X' &= -0.92 \pm 0.16 \pm 0.14 \text{ mrad} = -0.92 \pm 0.21 \text{ mrad} \end{aligned}$$

Because the point-wise steering coil corrections cancel the stray magnetic field and scale with momentum the average beam positions and angles have a small spread at the dipole.

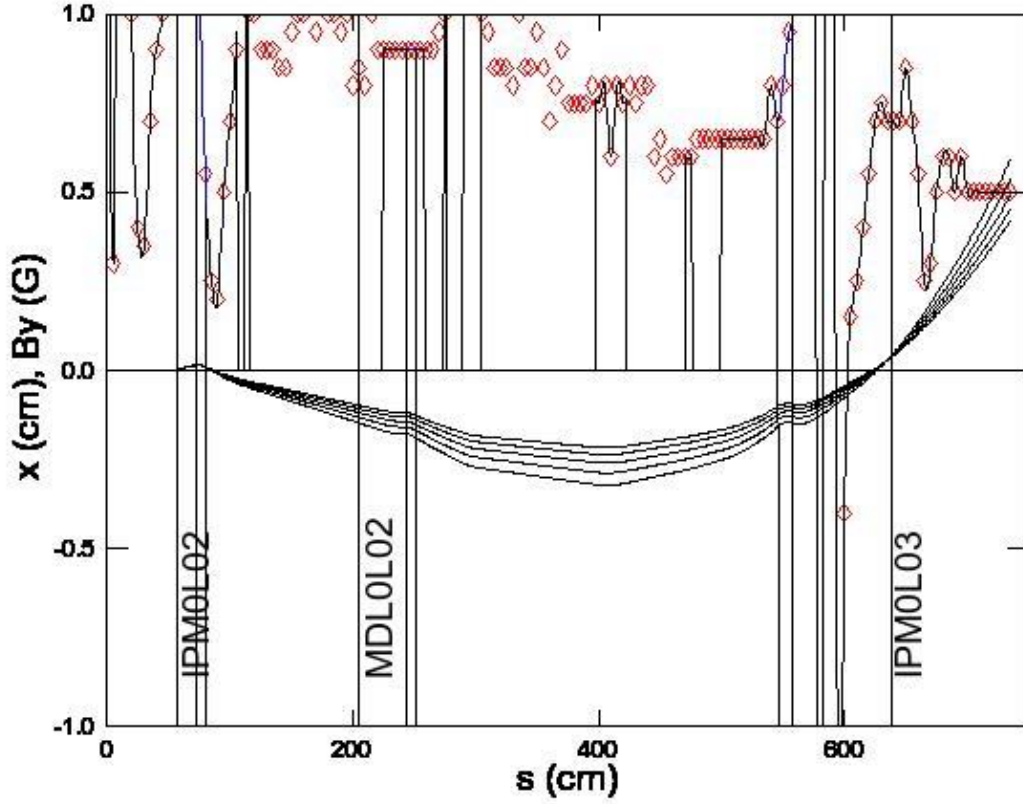


Fig. 5. The trajectories for 5 different momenta (4.5, 5.0, 5.5, 6.0, 6.5 MeV/c) with initial conditions IPM0L02 ($x=+0.07$ mm, $x'=+0.04$ mrad) is shown.

A survey of stray magnetic field for the 5D diagnostics beam line was also measured (see Appendix D) and is plotted in Fig. 5. Overlaid on this plot are trajectories (beginning at center of dipole) for the range of momenta using the model-calculated values at MDL0L02 ($x=-1.20$ mm, $x'=-0.92$ mrad).

Using the values calculated at MDL0L02 we continue tracking the beam through the 5D beam line to determine the additional deflection (adding or subtracting) required to produce the measured beam positions at IPM5D00 or IPM5D01,

$$\langle 5D00_COR \rangle_{meas} = 0.27 \pm 0.01 \pm 0.25 \pm 0.50 \text{ mm} = 0.27 \pm 0.56 \text{ mm}$$

$$\langle 5D01_COR \rangle_{meas} = 3.96 \pm 0.29 \pm 0.25 \pm 0.50 \text{ mm} = 3.96 \pm 0.63 \text{ mm}$$

The difference in deflection is attributed to the dipole bending the beam by an amount different than $+25.0^\circ$, that is, it is a correction to the ideal angular deflection. The results obtained by including the model value of MDL0L2 the following additional deflection for the two beam position monitors is determined,

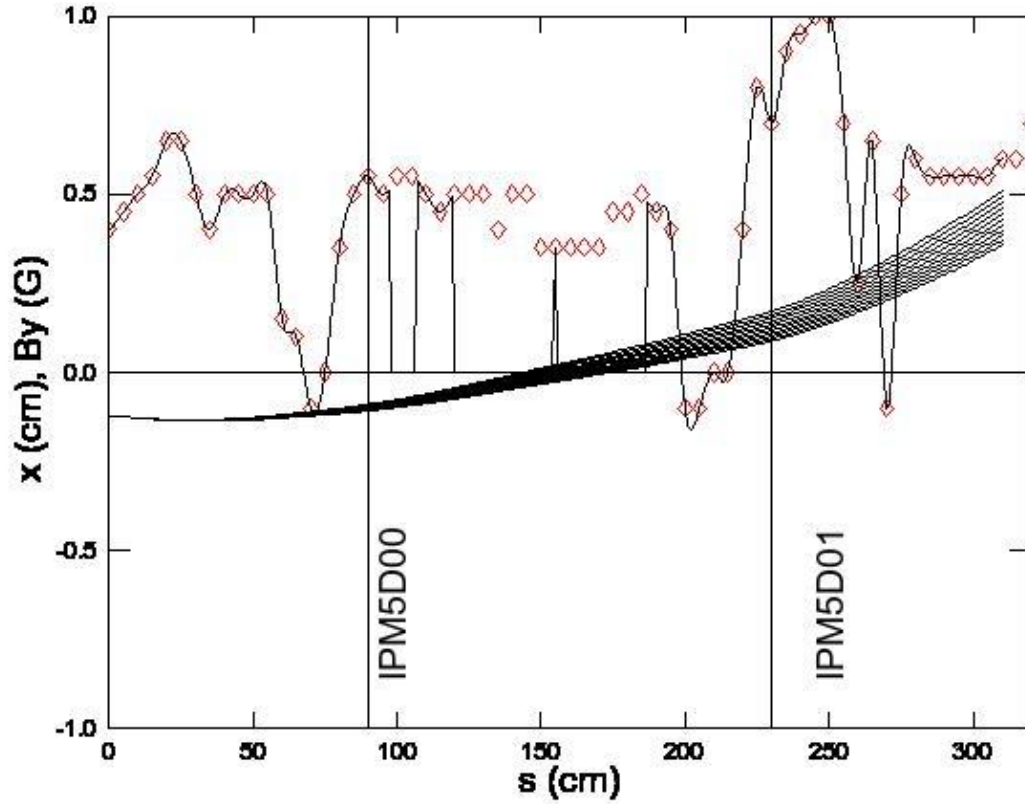


Fig. 5. The trajectories for 5 different momenta (4.5, 5.0, 5.5, 6.0, 6.5 MeV/c) with initial conditions MDL0L02 ($x = -1.20$ mm, $x' = -0.92$ mrad) is shown.

$$IPM5D00 \Rightarrow \theta = 1.43 \pm 0.90 \text{ mrad} = 0.0819^\circ \pm 0.0516^\circ$$

$$IPM5D01 \Rightarrow \theta = 1.30 \pm 0.28 \text{ mrad} = 0.0745^\circ \pm 0.0160^\circ$$

The uncertainty associated with IPM5D01 is smaller because this beam position monitor is further from the dipole magnet. The weighted average of the two measurements is finally,

$$\langle \theta \rangle = 1.311 \pm 0.267 \text{ mrad} = 0.0751^\circ \pm 0.015^\circ.$$

Summary

This note summarizes the Mott Run II beam energy measurements and discusses a method to calculate the beam momentum when including all of the magnetic fields (dipole, stray, steering coils). The method uses the TOSCA model to first calculate the beam momentum for an ideal 25.0° bend. The beam orbit is then modeled accounting for stray fields and steering coils, and bounded by beam position monitor measurements with realistic uncertainties. The model is used to determine the additional (positive or negative) deflection that must occur between the beam entering and exiting the dipole magnet. This additional deflection is attributed to

the dipole bending the beam more (lower momentum) or less (higher momentum) than assumed for the ideal bend.

This additional deflection computed suggests the dipole deflected the beam (independent of the orbit due to the initial conditions at IPM0L02, the stray field and the steering coils) by an amount $\langle\theta\rangle = 25.0751^\circ \pm 0.015^\circ$.

The dipole is powered with a standard 10 Amp trim power supply with reported [5] absolute calibration better than 5 mA. For Run II the dipole was operated with currents ranging approximately from 2800-3240 mA. If one considers only the trim power supply the contributing uncertainty is 0.18%. Additionally, a precision magnetic probe with accuracy 10^{-4} is mounted in the magnet gap to provide absolute calibration to the requested magnetic field. However, this value was not recorded and the probe has since been adjusted. Consequently, for Mott Run II the uncertainty associated with the power supply is used. A summary of the error budget is given in Table 4.

Table 4. Error budget for beam momentum method is listed.

Contribution	Value
TOSCA Model (Ref [4])	0.10%
Power Supply Calibration	0.18%
Model Correction	0.06%
Total	0.21%

The corrected beam momenta (P_C), kinetic energy (T) and uncertainties are computed according to the following relationships and reported in Table 5,

$$P_C = P_T (25.0/\langle\theta\rangle)$$

$$\delta T/T = (1-1/\gamma) \delta P_C/P_C$$

Table 5. Summary table.

Conditions		Momentum			Kinetic Energy	
R028	MDL0L02	TOSCA	Corrected		Final	
GSET	BL	p	p	dp	T	dT
MV/m	G-cm	MeV/c	MeV/c	MeV/c	MeV	MeV
3.350	7109.570	5.035	5.020	0.011	4.535	0.010
3.740	7384.340	5.229	5.213	0.011	4.727	0.011
4.120	7646.010	5.415	5.399	0.011	4.912	0.011
4.500	7927.590	5.614	5.597	0.012	5.109	0.012
4.890	8185.000	5.797	5.780	0.012	5.291	0.012

Reference

- [1] Jefferson Lab Alignment Group, *Data Transmittal #L1456*, May 25 2012 (note the information for magnets MQJ0L03 and MQJ0L03A appear reversed).
- [2] Jefferson Lab Alignment Group, *Data Transmittal #L1462 Rev. 2*, Jan 22 2013.
- [3] Magnet Measurement Facility, */u/group/MagTest/DataBase/DL*
- [4] J. Benesh, *"A detailed examination of the MDL field map and the TOSCA model of this "5 MeV" dipole"*, JLab-TN-15-017.
- [5] Private communication, Simon Wood testing 10A trim in IN02B26-9 (MDL0L02), July 2013.

Appendix A

The sequence of steps for each measurement is described here:

1. Setup beam to Faraday Cup #2
2. Quad center and update .SOF for IPM0L02, IPM0L03, IPM5D00, IPM5D01
3. Set MDL0L02 to zero and cycle
4. Set magnets on 2D and 3D lines to zero and cycle
5. Set skew and normal quads from IPM0L02 to IPM0L03 to zero and cycle
6. (Optional) Zero beam positions at IPM0L02 and IPM0L03
7. Record undeflected orbit conditions:
 - a. MDL0L02
 - b. beam positions IPM0L02/IPM0L03
 - c. all corrector settings in 0L line
8. Set steering coils (stray fields) between MDL0L02 and IPM0L03 to zero
9. Set MDL0L02 to deflect beam to IPM5D00 and IPM5D01 so both within 5mm.
10. Cycle MDL0L02 and iterate with step #9 until satisfied
11. Record deflected orbit conditions:
 - a. MDL0L02
 - b. beam positions IPM5D00/IPM5D01
 - c. all corrector settings in 5D line

Appendix B – Stray Magnetic Field 0L Region

The stray magnetic field between ITV0L02 and IFY0L03 was surveyed between Dec. 22, 2015 and Jan. 12, 2016. With magnets unpowered and degaussed the vertical component of stray magnetic field was measured every 5 cm both above and below the beam pipe and averaged. Additionally the upstream (US) and downstream (DS) location of beam line elements and regions of beam line that are covered in magnetic shielding were measured with an uncertainty of 0.5cm in a relative coordinate system.

The component and shielding positions are summarized first followed by magnetic field measurement results. The magnetic field measurement results are shown for Run II and following additional magnetic shielding added on January 12, 2016. The differences are noted in **red**.

<i>Element</i>	<i>US (cm)</i>	<i>DS (cm)</i>
ITV0L02/VIP0L02	1	1
MQJ0L02	22	33
IPM0L02	47	67
MQS0L02	54	67
MHB0L02	73	80
MQJ0L02A	83	94
IBC0L02	130	145
MDL0L02	199	209
MHB0L02A	244	251
MQS0L02B	398	410
MHB0L02B	413	419
MHE0L03V	513	525
MHE0L03H	527	540
MBH0L03	547	557
ITV0L03/VIP0L03	584	584
MQJ0L03A	602	613
IPM0L03	629	649
MQS0L03	636	649
MQJ0L03	665	676
IHA0L03	695	695
IFY0L03	732	732

<i>Mu-Metal</i>	<i>US (cm)</i>	<i>DS (cm)</i>
1	107	112
2	116	224
3	148	188
4	260	274
5	277	289
6	305	397
7	423	471
8	477	499

Z (cm)	Run II			After Jan 12, 2016		
	By_T (G)	By_B (G)	<By> (G)	By_T (G)	By_B (G)	<By> (G)
0	1.1	4.0	2.6	1.0	0.9	1.0
5	1.1	-0.5	0.3	1.0	0.8	0.9
10	2.0	3.0	2.5	0.9	0.9	0.9
15	2.2	3.0	2.6	0.7	0.7	0.7
20	1.0	1.0	1.0	1.0	1.0	1.0
25	0.5	0.3	0.4	0.5	0.3	0.4
30	0.2	0.5	0.4	0.2	0.5	0.4
35	0.7	0.7	0.7	0.7	0.7	0.7
40	0.9	0.9	0.9	0.9	0.9	0.9
45	0.9	1.1	1.0	0.9	1.1	1.0
50	1.1	1.2	1.2	1.1	1.2	1.2
55	1.1	1.1	1.1	1.1	1.1	1.1
60	1.0	1.1	1.1	1.0	1.1	1.1
65	1.3	1.2	1.3	1.3	1.2	1.3
70	1.1	1.2	1.2	1.1	1.2	1.2
75	1.1	1.0	1.1	1.1	1.0	1.1
80	0.5	0.6	0.6	0.5	0.6	0.6
85	0.2	0.3	0.3	0.2	0.3	0.3
90	0.2	0.2	0.2	0.2	0.2	0.2
95	0.5	0.5	0.5	0.5	0.5	0.5
100	0.7	0.7	0.7	0.7	0.7	0.7
105	0.9	0.9	0.9	0.9	0.9	0.9
110	1.1	1.1	1.1	1.1	1.1	1.1
115	1.0	1.0	1.0	1.0	1.0	1.0
120	0.9	1.1	1.0	0.9	1.1	1.0
125	0.9	0.9	0.9	0.9	0.9	0.9
130	0.9	0.9	0.9	0.9	0.9	0.9
135	0.9	0.9	0.9	0.9	0.9	0.9
140	0.9	0.8	0.9	0.9	0.8	0.9
145	0.9	0.8	0.9	0.9	0.8	0.9
150	1.0	0.9	1.0	1.0	0.9	1.0
155	1.1	0.9	1.0	1.1	0.9	1.0
160	1.0	1.0	1.0	1.0	1.0	1.0
165	1.1	1.1	1.1	1.1	1.1	1.1
170	1.0	0.9	1.0	1.0	0.9	1.0
175	1.0	1.1	1.1	1.0	1.1	1.1
180	1.0	1.0	1.0	1.0	1.0	1.0
185	1.0	1.0	1.0	1.0	1.0	1.0
190	0.9	1.0	1.0	0.9	1.0	1.0
195	1.0	1.0	1.0	1.0	1.0	1.0
200	0.7	0.9	0.8	0.7	0.9	0.8

205	0.8	0.9	0.9	0.8	0.9	0.9
210	0.8	0.8	0.8	0.8	0.8	0.8
215	1.0	1.0	1.0	1.0	1.0	1.0
220	0.9	0.9	0.9	0.9	0.9	0.9
225	0.9	0.9	0.9	0.9	0.9	0.9
230	0.9	0.9	0.9	0.9	0.9	0.9
235	0.9	0.9	0.9	0.9	0.9	0.9
240	0.9	0.9	0.9	0.9	0.9	0.9
245	0.9	0.9	0.9	0.9	0.9	0.9
250	0.9	0.9	0.9	0.9	0.9	0.9
255	0.9	0.9	0.9	0.9	0.9	0.9
260	0.9	0.9	0.9	0.9	0.9	0.9
265	0.9	0.9	0.9	0.9	0.9	0.9
270	0.9	1.0	1.0	0.9	1.0	1.0
275	0.9	1.1	1.0	0.9	1.1	1.0
280	1.0	1.1	1.1	1.0	1.1	1.1
285	1.0	1.2	1.1	1.0	1.2	1.1
290	1.2	1.1	1.2	1.2	1.1	1.2
295	1.7	1.0	1.4	1.7	1.0	1.4
300	1.2	1.1	1.2	1.2	1.1	1.2
305	1.0	1.0	1.0	1.0	1.0	1.0
310	0.9	1.0	1.0	0.9	1.0	1.0
315	0.8	0.9	0.9	0.8	0.9	0.9
320	0.9	0.8	0.9	0.9	0.8	0.9
325	0.9	0.8	0.9	0.9	0.8	0.9
330	0.9	0.7	0.8	0.9	0.7	0.8
335	1.0	1.0	1.0	1.0	1.0	1.0
340	0.9	0.8	0.9	0.9	0.8	0.9
345	0.8	0.9	0.9	0.8	0.9	0.9
350	0.9	1.0	1.0	0.9	1.0	1.0
355	0.8	0.9	0.9	0.8	0.9	0.9
360	0.6	0.8	0.7	0.6	0.8	0.7
365	0.8	0.8	0.8	0.8	0.8	0.8
370	0.9	0.9	0.9	0.9	0.9	0.9
375	0.7	0.8	0.8	0.7	0.8	0.8
380	0.7	0.8	0.8	0.7	0.8	0.8
385	0.7	0.8	0.8	0.7	0.8	0.8
390	0.8	0.7	0.8	0.8	0.7	0.8
395	0.9	0.7	0.8	0.9	0.7	0.8
400	0.9	0.6	0.8	0.9	0.6	0.8
405	0.9	0.7	0.8	0.9	0.7	0.8

410	0.7	0.5	0.6	0.7	0.5	0.6
415	0.9	0.7	0.8	0.9	0.7	0.8
420	0.8	0.7	0.8	0.8	0.7	0.8
425	0.9	0.7	0.8	0.9	0.7	0.8
430	0.8	0.7	0.8	0.8	0.7	0.8
435	0.9	0.7	0.8	0.9	0.7	0.8
440	0.9	0.7	0.8	0.9	0.7	0.8
445	0.7	0.5	0.6	0.7	0.5	0.6
450	0.7	0.6	0.7	0.7	0.6	0.7
455	0.6	0.5	0.6	0.6	0.5	0.6
460	0.7	0.5	0.6	0.7	0.5	0.6
465	0.6	0.6	0.6	0.6	0.6	0.6
470	0.6	0.6	0.6	0.6	0.6	0.6
475	0.6	0.6	0.6	0.6	0.6	0.6
480	0.7	0.6	0.7	0.7	0.6	0.7
485	0.7	0.6	0.7	0.7	0.6	0.7
490	0.7	0.6	0.7	0.7	0.6	0.7
495	0.7	0.6	0.7	0.7	0.6	0.7
500	0.7	0.6	0.7	0.7	0.6	0.7
505	0.7	0.6	0.7	0.7	0.6	0.7
510	0.7	0.6	0.7	0.7	0.6	0.7
515	0.7	0.6	0.7	0.7	0.6	0.7
520	0.7	0.6	0.7	0.7	0.6	0.7
525	0.7	0.6	0.7	0.7	0.6	0.7
530	0.7	0.6	0.7	0.7	0.6	0.7
535	0.7	0.6	0.7	0.7	0.6	0.7
540	0.9	0.7	0.8	0.9	0.7	0.8
545	0.8	0.6	0.7	0.8	0.6	0.7
550	0.9	0.7	0.8	0.9	0.7	0.8
555	1.0	0.9	1.0	0.8	0.6	0.7
560	1.3	1.2	1.3	0.8	0.6	0.7
565	1.7	3.2	2.5	0.5	0.5	0.5
570	1.8	4.2	3.0	0.5	0.5	0.5
575	1.5	4.6	3.1	0.5	0.7	0.6
580	1.0	-5.3	-2.2	0.5	0.5	0.5
585	0.6	3.9	2.3	0.5	0.6	0.6
590	0.1	3.6	1.9	0.6	0.9	0.8
595	-0.3	-2.0	-1.2	0.5	0.6	0.6
600	-0.2	-0.6	-0.4	0.4	0.4	0.4
605	0.0	0.3	0.2	0.0	0.3	0.2
610	0.3	0.2	0.3	0.3	0.2	0.3

615	0.3	0.5	0.4	0.3	0.5	0.4
620	0.6	0.5	0.6	0.6	0.5	0.6
625	0.7	0.7	0.7	0.7	0.7	0.7
630	0.8	0.7	0.8	0.8	0.7	0.8
635	0.7	0.7	0.7	0.7	0.7	0.7
640	0.7	0.7	0.7	0.7	0.7	0.7
645	0.7	0.7	0.7	0.7	0.7	0.7
650	0.8	0.9	0.9	0.8	0.9	0.9
655	0.7	0.7	0.7	0.7	0.7	0.7
660	0.6	0.5	0.6	0.6	0.5	0.6
665	0.3	0.2	0.3	0.3	0.2	0.3
670	0.3	0.3	0.3	0.3	0.3	0.3
675	0.5	0.5	0.5	0.5	0.5	0.5
680	0.6	0.6	0.6	0.6	0.6	0.6
685	0.6	0.6	0.6	0.6	0.6	0.6
690	0.5	0.5	0.5	0.5	0.5	0.5
695	0.7	0.5	0.6	0.7	0.5	0.6
700	0.5	0.5	0.5	0.5	0.5	0.5
705	0.5	0.5	0.5	0.5	0.5	0.5
710	0.5	0.5	0.5	0.5	0.5	0.5
715	0.5	0.5	0.5	0.5	0.5	0.5
720	0.5	0.5	0.5	0.5	0.5	0.5
725	0.5	0.5	0.5	0.5	0.5	0.5
730	0.5	0.5	0.5	0.5	0.5	0.5
735	0.5	0.5	0.5	0.5	0.5	0.5

Appendix C – Haimson Steering Magnet Calibration

In addition to the spectrometer dipole magnet two sizes (BH and HB) of Haimson-style steering coils were used to make point-wise corrections to compensate for the extended stray magnetic fields. The magnetic field profiles for both styles and both planes (horizontal or vertical) were measured at the Magnet Measurement Facility. Results for the four profiles are summarized in Table 2. A probe uncertainty of 0.05 Gauss for the 100-point profile results in an uncertainty of 2 G-m.

Table 2. The standard configuration at CEBAF is the inner coils produce horizontal (H) deflection and outer coils produce vertical (V) deflection.

Haimson Part No.	<i>JLab Type</i>	<i>Integrated Dipole Field (G-cm/A)</i>	<i>Integrated Dipole Field Uncertainty (G-cm)</i>
334	BH-Horizontal	179	2
335	BH-Vertical	143	2
825	HB-Horizontal	173	2
826	HB-Vertical	148	2

Appendix D– Stray Magnetic Field 5D Region

The stray magnetic field between MDL0L02 and IDL5D01 was surveyed between Dec. 21-23, 2015. With magnets unpowered and degaussed the vertical component of stray magnetic field was measured every 5 cm both above and below the beam pipe and averaged. Additionally the upstream (US) and downstream (DS) location of beam line elements and regions of beam line that are covered in magnetic shielding were measured with an uncertainty of 0.5cm in a relative coordinate system.

The component and shielding positions are summarized first followed by magnetic field measurement results. The magnetic field measurement results are shown for both Run II.

<i>Element Name</i>	<i>US (cm)</i>	<i>DS (cm)</i>
MDL0L02	20	20
MBH5D00	37	47
ITV5D00	62	62
MQD5D00	77.5	99.5
IPM5D00	102	116
MBH5D00A	104	115
MQD5D01	217.5	239.5
IPM5D01	242	256
MBH5D01	244	254
IFY5D01/ITV5D01	281	281
MBH5D01A	304	314
IDL5D01	340	349

<i>Mu-Metal</i>	<i>US (cm)</i>	<i>DS (cm)</i>
1	118	126
2	140	174
3	175.5	206.5

<i>Z (cm)</i>	<i>Run II</i>		
	<i>By_T (G)</i>	<i>By_B (G)</i>	<i><By> (G)</i>
0	0.40	0.40	0.40
5	0.50	0.40	0.45
10	0.50	0.50	0.50
15	0.60	0.50	0.55
20	0.70	0.60	0.65
25	0.70	0.60	0.65
30	0.50	0.50	0.50
35	0.40	0.40	0.40
40	0.50	0.50	0.50
45	0.50	0.50	0.50

50	0.50	0.50	0.50
55	0.50	0.50	0.50
60	0.10	0.20	0.15
65	0.10	0.10	0.10
70	-0.10	-0.10	-0.10
75	0.00	0.00	0.00
80	0.30	0.40	0.35
85	0.50	0.50	0.50
90	0.60	0.50	0.55
95	0.50	0.50	0.50
100	0.50	0.60	0.55
105	0.50	0.60	0.55
110	0.50	0.50	0.50
115	0.50	0.40	0.45
120	0.40	0.60	0.50
125	0.50	0.50	0.50
130	0.50	0.50	0.50
135	0.40	0.40	0.40
140	0.50	0.50	0.50
145	0.50	0.50	0.50
150	0.50	0.20	0.35
155	0.50	0.20	0.35
160	0.50	0.20	0.35
165	0.50	0.20	0.35
170	0.50	0.20	0.35
175	0.50	0.40	0.45
180	0.50	0.40	0.45
185	0.40	0.60	0.50
190	0.50	0.40	0.45
195	0.40	0.40	0.40
200	-0.20	0.00	-0.10
205	-0.10	-0.10	-0.10
210	0.00	0.00	0.00
215	0.00	0.00	0.00
220	0.40	0.40	0.40
225	0.80	0.80	0.80
230	0.80	0.60	0.70
235	0.90	0.90	0.90
240	0.90	1.00	0.95
245	1.00	1.00	1.00
250	1.00	1.00	1.00

255	0.70	0.70	0.70
260	0.00	0.50	0.25
265	-0.40	1.70	0.65
270	-0.40	0.20	-0.10
275	0.50	0.50	0.50
280	0.60	0.60	0.60
285	0.60	0.50	0.55
290	0.60	0.50	0.55
295	0.60	0.50	0.55
300	0.60	0.50	0.55
305	0.60	0.50	0.55
310	0.60	0.60	0.60
315	0.60	0.60	0.60
320	0.70	0.70	0.70
325	0.70	0.70	0.70
330	0.70	0.70	0.70